Journal of Science-FAS-SEUSL (2025) [Volume 06, No.1]

ISSN: 2738-2184

Influence of spin layers and anisotropic interactions on magnetic energy in ferromagnetic films via fourth order Heisenberg Hamiltonian

M.S.M. Farhan[a*] and P. Samarasekara[b]

[a]Department of Physical Science, Trincomalee Campus, Eastern University, Sri Lanka.

[b]Department of Physics, University of Peradeniya, Peradeniya, Sri Lanka.

[*]farhanmsm@esn.ac.lk

Abstract

This study examines the behaviour of magnetic energy in ferromagnetic thin films, focusing on spin interactions and anisotropy effects across different parameter configurations. Using the Heisenberg Hamiltonian model, we explored how various magnetic factors including spin exchange, dipole interactions, and second- and fourth-order magnetic anisotropies, influence the total energy in simple cubic lattices with two spin layers. Key findings reveal that higher-order terms in the Hamiltonian significantly increase magnetic energy, with major energy peaks observed around specific values of $\frac{J}{\omega}$, notably at approximately 6 and 74, depending on the parameter configurations. Detailed visual analyses through 2D and 3D plots illustrate the relationships between spin exchange interactions, spin angles, and energy, providing insights into points of stability and resonance within the films. Additionally, we found that a stronger second-order anisotropy compared to fourth-order leads to significantly higher magnetic energy, which has potential applications in the development of efficient permanent magnets. By clarifying the impact of anisotropies and spin interactions on magnetic energy, this research enhances our understanding of magnetic interactions in ferromagnetic films and offers practical guidance for designing advanced materials for use in magnetic memory devices, permanent magnets, and other applications requiring high-performance magnetic materials.

Keywords: Fourth order, Spin exchange interaction, Spin layers, Ferromagnetic thin films, Azimuthal angle, Magnetic energy

ISSN: 2738-2184

Introduction

Ferromagnetic films are important for magnetic memory devices and microwave technologies. Their performance is influenced by how easily they can be magnetized in different directions. Understanding these directions is key to improving the efficiency of devices that use these films. Various models have been used to study these films, such as Monte Carlo simulations for magnetic behaviour [1], the Ising model for layered films [2], and first-principles theories for alloys like FeCo [3]. The Korringa-Kohn-Rostoker method has also been used to analyse nickel on copper layers [4].

A common challenge in studying ferromagnetic films is that the observed magnetic properties often don't match theoretical predictions. This can happen due to overlapping electron shells that complicate the results. Additionally, during processes like annealing, stress-induced magnetic anisotropy (Ks) occurs because of differences in thermal expansion between the film and its substrate. This is especially important in soft magnetic materials, as it greatly affects coercivity and overall magnetic performance [5].

In our research, we explored the magnetic properties of both ferromagnetic and ferrite thin and thick films [6-13]. We used the classical Heisenberg Hamiltonian to analyse the total energy of these films, considering various factors such as magnetic energy, spin interactions, and higher-order magnetic effects. We present a specialized form of the Heisenberg Hamiltonian that incorporates several magnetic energy parameters for simple cubic structures with two layers of spins. These parameters include spin dipole interaction, spin exchange interaction, second-order and fourth-order magnetic anisotropies, as well as demagnetization factors.

To help visualize our findings, we use MATLAB to create 2D and 3D graphs that show the relationships between energy, spin exchange interactions, and the angles of the spins. These visualizations improve our understanding of how these interactions work and offer insights for designing better ferromagnetic films for practical uses.

Overall, this study aims to enhance our knowledge of ferromagnetic films, emphasizing the importance of various interactions and anisotropies. By addressing the complexities of their behaviour, we contribute to the development of magnetic materials that are essential for future technologies.

Model

The Heisenberg Hamiltonian of ferromagnetic films can be formulated as following [8-10].

$$H = -\frac{J}{2}\sum_{m,n}\vec{S}_m.\vec{S}_n + \frac{\omega}{2}\sum_{m\neq n}\left(\frac{\vec{S}_m.\vec{S}_n}{r_{mn}^3} - \frac{3(\vec{S}_m.\vec{r}_{mn})(\vec{r}_{mn}.\vec{S}_n)}{r_{mn}^5}\right) - \sum_m D_{\lambda_m}^{(2)}(S_m^z)^2$$
$$-\sum_m D_{\lambda_m}^{(4)}(S_m^z)^4 - \sum_{m,n}[\vec{H} - (N_d\vec{S}_n/\mu_0)].\vec{S}_m - \sum_m K_s \sin 2\theta_m \qquad (1)$$

Here $\vec{S}_m$ and $\vec{S}_n$ are two spins. Above equation can be simplified into following form

ISSN: 2738-2184

$$E(\theta) = -\frac{1}{2}\sum_{m,n=1}^{N}\left[\left(JZ_{|m-n|} - \frac{\omega}{4}\Phi_{|m-n|}\right)\cos(\theta_m - \theta_n) - \frac{3\omega}{4}\Phi_{|m-n|}\cos(\theta_m + \theta_n)\right]$$

$$-\sum_{m=1}^{N}(D_m^{(2)}cos^2\theta_m + D_m^{(4)}cos^4\theta_m + H_{in}sin\theta_m + H_{out}cos\theta_m)$$

$$+\sum_{m,n=1}^{N}\frac{N_d}{\mu_0}cos(\theta_m - \theta_n) - K_s\sum_{m=1}^{N}sin2\theta_m \quad (2)$$

Here N, $m\,(or\ n)$, J, $Z_{|m-n|}$, ω, $\Phi_{|m-n|}$, $\theta_m(\theta_n)$, $D_m^{(2)}$, $D_m^{(4)}$, H_{in}, H_{out}, N_d and K_s are total number of layers, layer index, spin exchange interaction, number of nearest spin neighbors, strength of long range dipole interaction, partial summations of dipole interaction, azimuthal angles of spins, second and fourth order anisotropy constants, in plane and out of plane applied magnetic fields, demagnetization factor and stress induced anisotropy constants respectively.

The spin structure is considered to be slightly disoriented. Therefore, the spins could be considered to have angles distributed about an average angle θ. By choosing azimuthal angles as

$$\theta_m = \theta + \varepsilon_m \text{ and } \theta_n = \theta + \varepsilon_n \quad (3)$$

Where the ε's are small positive or negative angular deviations.

Then, $\theta_m - \theta_n = \varepsilon_m - \varepsilon_n$ and $\theta_m + \theta_n = 2\theta + \varepsilon_m + \varepsilon_n$. After substituting these new angles in above equation number (1), the cosine and sine terms can be expanded up to the fourth order of ε_m and ε_n as following.

$$E(\theta) = E_0 + E(\varepsilon) + E(\varepsilon^2) + E(\varepsilon^3) + E(\varepsilon^4) + \ldots\ldots\ldots\ldots \quad (4)$$

If the fifth and higher order perturbations are neglected, then

$$E(\theta) = E_0 + E(\varepsilon) + E(\varepsilon^2) + E(\varepsilon^3) + E(\varepsilon^4) \quad (5)$$

Here

$$E_0 = -\frac{1}{2}\sum_{m,n=1}^{N}\left(JZ_{|m-n|} - \frac{\omega}{4}\Phi_{|m-n|}\right) + \frac{3\omega}{8}cos2\theta\sum_{m,n=1}^{N}\Phi_{|m-n|} - cos^2\theta\sum_{m=1}^{N}D_m^{(2)}$$

$$-cos^4\theta\sum_{m=1}^{N}D_m^{(4)} - N(H_{in}sin\theta + H_{out}cos\theta + K_s sin2\theta) + \frac{N_d N^2}{\mu_0} \quad (6)$$

$$E(\varepsilon) = -\frac{3\omega}{8}sin2\theta\sum_{m,n=1}^{N}\Phi_{|m-n|}(\varepsilon_m + \varepsilon_n) + sin2\theta\sum_{m=1}^{N}D_m^{(2)}\varepsilon_m$$

ISSN: 2738-2184

$$+2cos^2\theta sin2\theta\sum_{m=1}^{N}D_m^{(4)}\varepsilon_m - H_{in}cos\theta\sum_{m=1}^{N}\varepsilon_m + H_{out}sin\theta\sum_{m=1}^{N}\varepsilon_m$$

$$-2K_s cos2\theta\sum_{m=1}^{N}\varepsilon_m \tag{7}$$

$$E(\varepsilon^2) = \frac{1}{4}\sum_{m,n=1}^{N}\left(JZ_{|m-n|} - \frac{\omega}{4}\Phi_{|m-n|}\right)(\varepsilon_m - \varepsilon_n)^2 - \frac{3\omega}{16}cos2\theta\sum_{m,n=1}^{N}\Phi_{|m-n|}(\varepsilon_m + \varepsilon_n)^2$$

$$+cos2\theta\sum_{m=1}^{N}D_m^{(2)}\varepsilon_m^2 + 2cos^2\theta(cos^2\theta - 3sin^2\theta)\sum_{m=1}^{N}D_m^{(4)}\varepsilon_m^2 + \frac{H_{in}}{2}sin\theta\sum_{m=1}^{N}\varepsilon_m^2$$

$$+\frac{H_{out}}{2}cos\theta\sum_{m=1}^{N}\varepsilon_m^2 - \frac{N_d}{2\mu_0}\sum_{m,n=1}^{N}(\varepsilon_m - \varepsilon_n)^2 + 2K_s sin2\theta\sum_{m=1}^{N}\varepsilon_m^2 \tag{8}$$

$$E(\varepsilon^3) = \frac{\omega}{16}sin2\theta\sum_{m,n=1}^{N}\Phi_{|m-n|}(\varepsilon_m + \varepsilon_n)^3 - \frac{4}{3}sin\theta cos\theta\sum_{m=1}^{N}D_m^{(2)}\varepsilon_m^3$$

$$-4sin\theta cos\theta\left(\frac{5}{3}cos^2\theta - sin^2\theta\right)\sum_{m=1}^{N}D_m^{(4)}\varepsilon_m^3 + \frac{H_{in}}{6}cos\theta\sum_{m=1}^{N}\varepsilon_m^3$$

$$-\frac{H_{out}}{6}sin\theta\sum_{m=1}^{N}\varepsilon_m^3 + \frac{4}{3}K_s cos2\theta\sum_{m=1}^{N}\varepsilon_m^3 \tag{9}$$

$$E(\varepsilon^4) = -\frac{1}{48}\sum_{m,n=1}^{N}\left(JZ_{|m-n|} - \frac{\omega}{4}\Phi_{|m-n|}\right)(\varepsilon_m - \varepsilon_n)^4 + \frac{\omega}{64}cos2\theta\sum_{m,n=1}^{N}\Phi_{|m-n|}(\varepsilon_m + \varepsilon_n)^4$$

$$-\frac{1}{3}cos2\theta\sum_{m=1}^{N}D_m^{(2)}\varepsilon_m^4 - (\frac{5}{3}cos^4\theta - 8cos^2\theta sin^2\theta + sin^4\theta)\sum_{m=1}^{N}D_m^{(4)}\varepsilon_m^4$$

$$-\frac{H_{in}}{24}sin\theta\sum_{m=1}^{N}\varepsilon_m^4 - \frac{H_{out}}{24}cos\theta\sum_{m=1}^{N}\varepsilon_m^4 + \frac{N_d}{24\mu_0}\sum_{m,n=1}^{N}(\varepsilon_m - \varepsilon_n)^4$$

$$+\frac{2}{3}K_s sin2\theta\sum_{m=1}^{N}\varepsilon_m^4 \tag{10}$$

For films with two spin layers, N = 2. Therefore, m and n change from 1 to 2.

$$E_0 = -JZ_0 + \frac{\omega}{4}\Phi_0 - JZ_1 + \frac{\omega}{4}\Phi_1 + \frac{3\omega}{4}cos2\theta(\Phi_0 + \Phi_1) - cos^2\theta\left(D_1^{(2)} + D_2^{(2)}\right)$$

$$-cos^4\theta\left(D_1^{(4)} + D_2^{(4)}\right) - 2(H_{in}sin\theta + H_{out}cos\theta + K_s sin2\theta) + \frac{4N_d}{\mu_0} \tag{11}$$

$$E(\varepsilon) = -\frac{3\omega}{4}sin2\theta[(\Phi_0 + \Phi_1)(\varepsilon_1 + \varepsilon_2)] + sin2\theta\left(D_1^{(2)}\varepsilon_1 + D_2^{(2)}\varepsilon_2\right)$$

$$+2cos^2\theta sin2\theta\left(D_1^{(4)}\varepsilon_1 + D_2^{(4)}\varepsilon_2\right) - H_{in}cos\theta(\varepsilon_1 + \varepsilon_2) + H_{out}sin\theta(\varepsilon_1 + \varepsilon_2)$$

$$-2K_s cos2\theta(\varepsilon_1 + \varepsilon_2) \tag{12}$$

$$E(\varepsilon^2) = \frac{1}{2}\left(JZ_1 - \frac{\omega}{4}\Phi_1\right)(\varepsilon_1 - \varepsilon_2)^2 - \frac{3\omega}{8}cos2\theta[2\Phi_0({\varepsilon_1}^2 + {\varepsilon_2}^2) + \Phi_1(\varepsilon_1 + \varepsilon_2)^2]$$

$$+cos2\theta\left(D_1^{(2)}{\varepsilon_1}^2 + D_2^{(2)}{\varepsilon_2}^2\right) + 2cos^2\theta(cos^2\theta - 3sin^2\theta)\left(D_1^{(4)}{\varepsilon_1}^2 + D_2^{(4)}{\varepsilon_2}^2\right)$$

$$+\frac{H_{in}}{2}sin\theta({\varepsilon_1}^2 + {\varepsilon_2}^2) + \frac{H_{out}}{2}cos\theta({\varepsilon_1}^2 + {\varepsilon_2}^2) - \frac{N_d}{\mu_0}(\varepsilon_1 - \varepsilon_2)^2$$

$$+2K_s sin2\theta({\varepsilon_1}^2 + {\varepsilon_2}^2) \tag{13}$$

$$E(\varepsilon^3) = \frac{\omega}{8}sin2\theta[4\Phi_0({\varepsilon_1}^3 + {\varepsilon_2}^3) + \Phi_1(\varepsilon_1 + \varepsilon_2)^3] - \frac{4}{3}sin\theta cos\theta\left(D_1^{(2)}{\varepsilon_1}^3 + D_2^{(2)}{\varepsilon_2}^3\right)$$

$$-4sin\theta cos\theta\left(\frac{5}{3}cos^2\theta - sin^2\theta\right)\left(D_1^{(4)}{\varepsilon_1}^3 + D_2^{(4)}{\varepsilon_2}^3\right) + \frac{H_{in}}{6}cos\theta({\varepsilon_1}^3 + {\varepsilon_2}^3)$$

$$-\frac{H_{out}}{6}sin\theta({\varepsilon_1}^3 + {\varepsilon_2}^3) + \frac{4}{3}K_s cos2\theta({\varepsilon_1}^3 + {\varepsilon_2}^3) \tag{14}$$

$$E(\varepsilon^4) = -\frac{1}{24}\left(JZ_1 - \frac{\omega}{4}\Phi_1\right)(\varepsilon_1 - \varepsilon_2)^4 + \frac{\omega}{32}cos2\theta[8\Phi_0({\varepsilon_1}^4 + {\varepsilon_2}^4) + \Phi_1(\varepsilon_1 + \varepsilon_2)^4]$$

$$-\frac{1}{3}cos2\theta\left(D_1^{(2)}{\varepsilon_1}^4 + D_2^{(2)}{\varepsilon_2}^4\right) - (\frac{5}{3}cos^4\theta - 8cos^2\theta sin^2\theta$$

$$+sin^4\theta)\left(D_1^{(4)}{\varepsilon_1}^4 + D_2^{(4)}{\varepsilon_2}^4\right) - \frac{H_{in}}{24}sin\theta({\varepsilon_1}^4 + {\varepsilon_2}^4) - \frac{H_{out}}{24}cos\theta({\varepsilon_1}^4 + {\varepsilon_2}^4)$$

$$+\frac{N_d}{12\mu_0}(\varepsilon_1 - \varepsilon_2)^4 - \frac{2}{3}K_s sin2\theta({\varepsilon_1}^4 + {\varepsilon_2}^4) \tag{15}$$

First (α), second (C), third (β) and fourth $(F\ and\ G)$ order perturbation term can be found in terms of a row and column matrix with all seven terms. Then, the total magnetic energy in equation (2) can be deduced to

$$E(\theta) = E_0 + \vec{\alpha}.\vec{\varepsilon} + \tfrac{1}{2}\vec{\varepsilon}.C.\vec{\varepsilon} + \varepsilon^2.\beta.\vec{\varepsilon} + \varepsilon^3.F.\vec{\varepsilon} + \varepsilon^2.G.\varepsilon^2 \tag{16}$$

ISSN: 2738-2184

For the minimum energy of the second order perturbed term

$$\vec{\varepsilon} = -C^{+}.\alpha \tag{17}$$

Here C^{+} is the pseudo inverse of matrix C. C^{+} can be found using

$$C.C^{+} = 1 - \frac{E}{N} \tag{18}$$

Here E is the matrix with all elements given $by\ E_{mn} = 1$. 1 is the identity matrix.

Therefore,

$$C_{11}^{+} = C_{22}^{+} = \frac{C_{21} + C_{22}}{2(C_{11}C_{22} - C_{21}^{2})} \tag{19}$$

$$C_{12}^{+} = C_{21}^{+} = \frac{C_{21} + C_{22}}{2(C_{21}^{2} - C_{11}C_{22})} \tag{20}$$

Therefore, from the matrix equation (17)

$$\varepsilon_1 = (\alpha_2 - \alpha_1)\ C_{11}^{+} \tag{21}$$

$$\varepsilon_2 = (\alpha_2 - \alpha_1)\ C_{21}^{+} \tag{22}$$

After substituting ε in equation (16), the total magnetic energy can be determined.

Results and Discussion

All the graphs in this manuscript were plotted for ferromagnetic films with simple cubic lattice and two spin layers. For ferromagnetic films with Sc (001) structure, Z_0=4, Z_1=1, Z_2=0, Φ_0 =9.0336 and $\Phi_1 = -0.3275$ [14-16]. 3D plot of energy versus angle and Spin exchange interaction is given in figure 1 for $\frac{D_1^{(4)}}{\omega} = 5$ and $\frac{D_2^{(4)}}{\omega} = 10$. Here other parameters are fixed at $\frac{Ks}{\omega} = \frac{H_{in}}{\omega} = \frac{H_{out}}{\omega} = \frac{N_d}{\mu_0 \omega} = \frac{D_1^{(2)}}{\omega} = \frac{D_2^{(2)}}{\omega} = 10$ for this simulation. The peaks along the direction of angle are closely packed compared to the second and third order perturbed cases [9, 12, 17-19]. The cross section of this 3D plot at one particular angle is given at figure 3.2. By rotating 3D plot in figure 1, figure 2 can be obtained. Energy maximums can be observed at $\frac{J}{\omega} = 6, 63, 74, 90, ..\ etc.$ The major maximum observed at about $\frac{J}{\omega} = 74$. Energy in these graphs is in the order of 10^{42}. The order of the energy in this case is higher the total magnetic energy (10^{13}) obtained using the fourth order perturbed Heisenberg Hamiltonian with spin exchange interaction, second order anisotropy terms only [20]. It implies that introducing more terms to Heisenberg Hamiltonian increases the total magnetic energy.

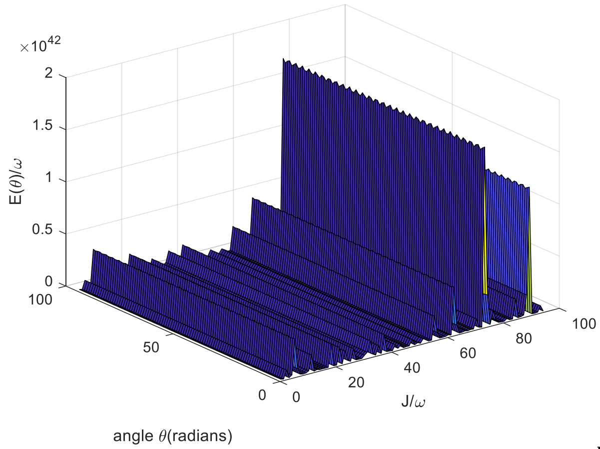

Figure 1: 3D plot of energy versus angle and spin exchange interaction for $\frac{D_1^{(4)}}{\omega} = 5$ and $\frac{D_2^{(4)}}{\omega} = 10$.

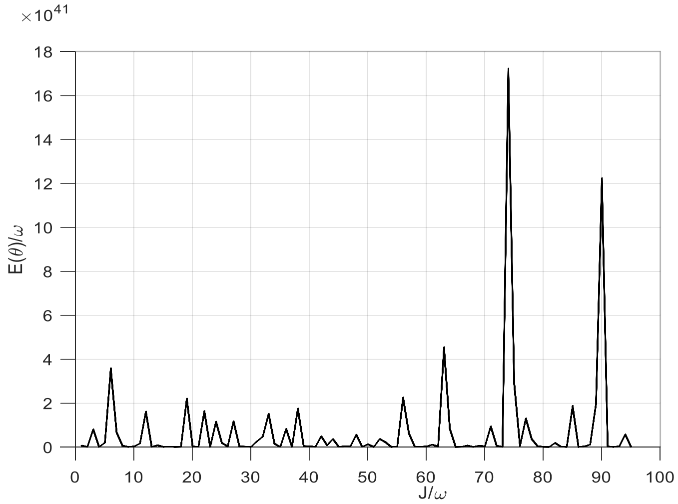

Figure 2: Graph of energy versus spin exchange interaction

Figure 3 shows the graph of energy versus angle for $\frac{J}{\omega} = 74$. Other parameters were kept at the values given above. In this graph, energy maximum can be observed at 5.843 radians and energy minimum cannot be found.

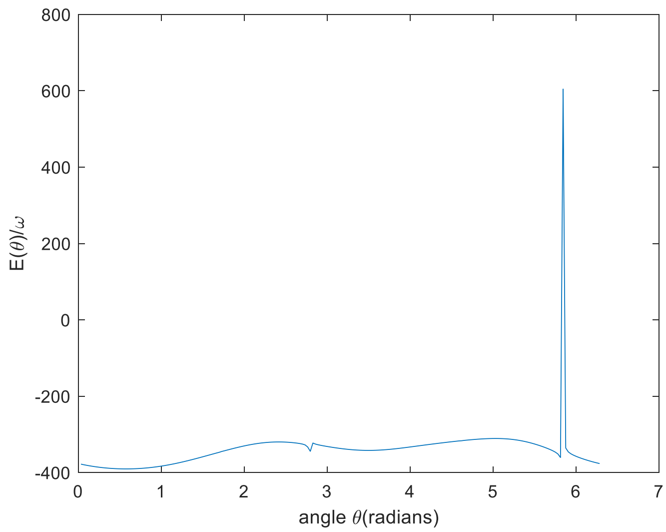

Figure 3: 2D graph of energy versus angle for $\frac{J}{\omega} = 74$.

3D plot of energy versus angle and spin exchange interaction is given in figure 4 for $\frac{D_1^{(4)}}{\omega} = 10$ and $\frac{D_2^{(4)}}{\omega} = 5$. Here other parameters are fixed at $\frac{H_{in}}{\omega} = \frac{H_{out}}{\omega} = \frac{N_d}{\mu_0 \omega} = \frac{D_1^{(2)}}{\omega} = \frac{D_2^{(2)}}{\omega} = \frac{K_s}{\omega} = 10$ for this simulation. In this graph, the energy maximums can be observed at $\frac{J}{\omega} = 6, 13, 25, 49, 74 \, .. etc$. The major maximum observed at about $\frac{J}{\omega} = 6$. Several peaks can be observed in both graphs. However, the gap between two peaks is not a constant. In addition, the magnetic energy increases from 10^{42} to 10^{43} when the values of both spin layers are interchanged. The energy of ferromagnetic thin films found using third order perturbed Heisenberg Hamiltonian was in the range of 10^{16} to 10^{19} [21].

Figure 5 represents the graph of energy versus angle for $\frac{J}{\omega} = 6$. Other parameters were kept at the values given above. In this graph, energy maximum can be observed at 0.6912 radians and energy minimum was found at 3.55 radians. This 2D graph is different from the graph obtained in figure 3.

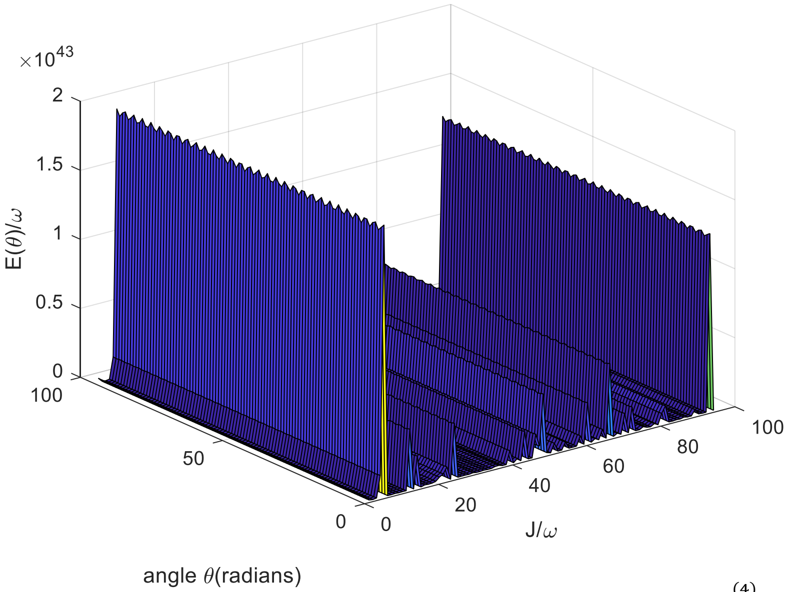

Figure 4: 3D plot of energy versus angle and spin exchange interaction for $\frac{D_1^{(4)}}{\omega} = 10$ and $\frac{D_2^{(4)}}{\omega} = 5$.

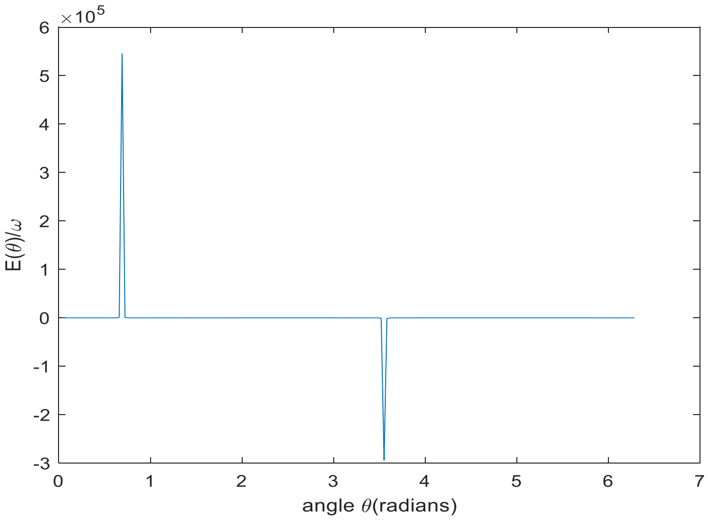

Figure 5: 2D graph of energy versus angle for $\frac{J}{\omega} = 6$.

3D plot of energy versus angle and spin exchange interaction is given in figure 6 for $\frac{D_1^{(2)}}{\omega} = 100$ and $\frac{D_2^{(2)}}{\omega} = 200$. Here other parameters are fixed at $\frac{H_{in}}{\omega} = \frac{H_{out}}{\omega} = \frac{N_d}{\mu_0 \omega} = \frac{D_1^{(4)}}{\omega} = \frac{D_2^{(4)}}{\omega} = \frac{K_s}{\omega} = 10$ for this simulation. In this graph, the energy maximums can be observed at $\frac{J}{\omega} = 11, 20, 45, 71, 93 \ldots etc$. The major maximum observed at about $\frac{J}{\omega} = 11$. Energy is in the order of 10^{52}. When the second order magnetic anisotropy is much higher than the fourth order magnetic anisotropy, the magnetic energy is high. These types of films find potential applications in permanent magnets.

Figure 7 shows the graph of energy versus angle at $\frac{J}{\omega} = 11$. Energy maxima of the graph can be observed at 0.8482, 2.513, 3.896 and 5.655 radians. The major maximum observed at 2.513 radians. Energy minima cannot be found in this graph.

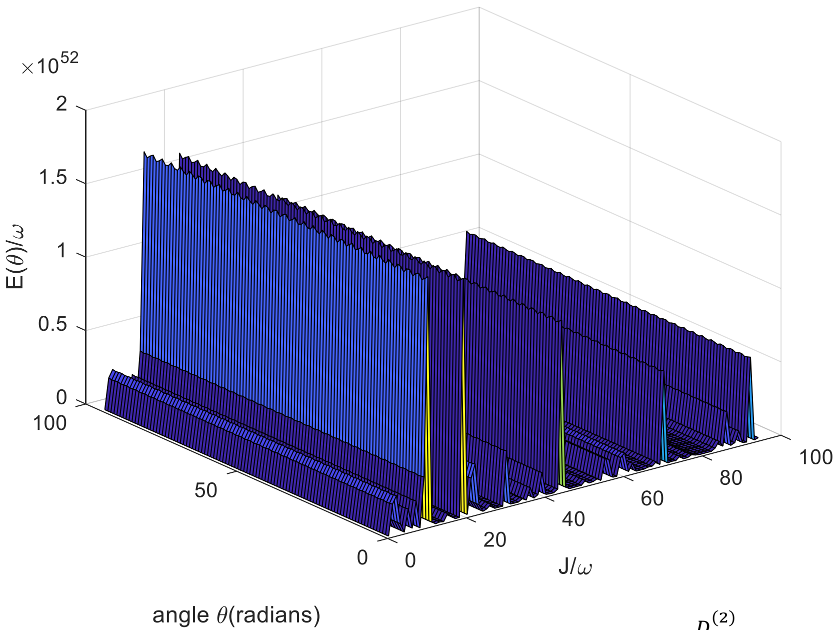

Figure 6: 3D plot of energy versus angle and spin exchange interaction for $\frac{D_1^{(2)}}{\omega} = 100$ and $\frac{D_2^{(2)}}{\omega} = 200$

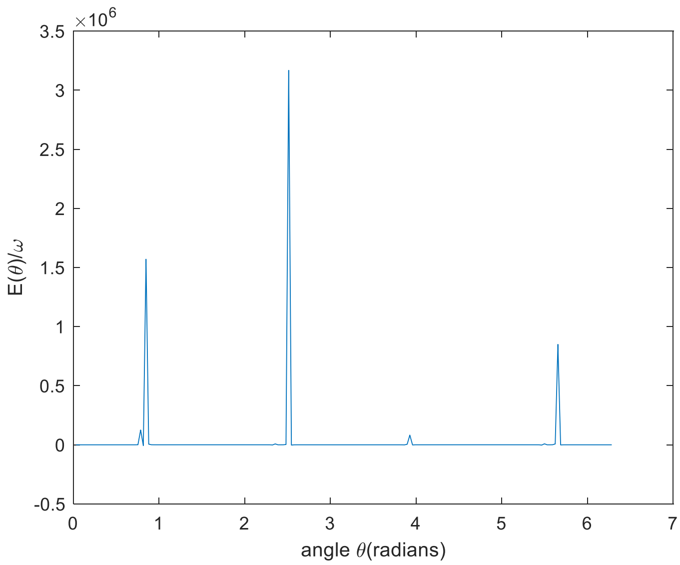

Figure 7: 2D graph of energy versus angle for $\frac{J}{\omega} = 11$.

Conclusion

This study investigated the magnetic properties of ferromagnetic and ferrite thin and thick films, particularly focusing on energy variations due to spin interactions and anisotropies in simple cubic lattices with two spin layers. By employing the Heisenberg Hamiltonian, we explored how different magnetic parameters, including spin exchange interactions, spin dipole interactions, and second- and fourth-order magnetic anisotropies, impact total magnetic energy. Key findings indicate that the inclusion of higher-order terms in the Heisenberg Hamiltonian raises the magnetic energy, as seen in energy peaks that occur at different values of $\frac{J}{\omega}$ across various parameter configurations. Notably, we observed that when fourth-order anisotropy terms are included alongside second-order terms, there is a significant increase in the total magnetic energy compared to third-order models, which aligns with theoretical expectations for such materials. The visualizations generated in this research, including 2D and 3D plots, reveal crucial energy peaks at different spin angles, with the highest energy peaks indicating potential points of stability or resonance within the material. For instance, major energy maxima were found at approximately $\frac{J}{\omega} = 74$ and $\frac{J}{\omega} = 6$, depending on the spin anisotropy configuration. Additionally, we identified that larger second-order anisotropy leads to increased magnetic energy, especially relevant in designing materials for applications such as permanent magnets. Overall, our work provides insight into the impact of anisotropies and spin interactions on magnetic energy in ferromagnetic films. These findings contribute to the development of advanced magnetic materials with optimized energy properties, which could enhance the efficiency and performance of technologies such as magnetic memory devices and permanent magnets.

References

1. Zhao, D., Feng Liu, Huber, D.L., Lagally, M.G. (2002). Step-induced magnetic-hystersis anisotropy in ferromagnetic thin films. Journal of Applied Physics, 91(5), 3150.
2. Bentaleb, M., Aouad El, N., Saber, M. (2002). Phase diagram of spin 1/2 Ising semi-infinite and film ferromagnets with spin 3/2 overlayers. Chinese Journal of Physics, 40(3), 307.
3. Spisak, D., Hafner, J. (2005). Theoretical study of FeCo/W (110) surface alloys. Journal of Magnetism and Magnetic Materials, 286, 386.
4. Ernst, A., Lueders, M., Temmerman, W.M., Szotek, Z., Van der Laan, G. (2000). Theoretical study of magnetic layers of nickel on copper; dead or alive? Journal of Physics: Condensed Matter, 12(26), 5599.
5. Samarasekara, P., Cadieu, F.J. (2001). Magnetic and structural properties of RF sputtered polycrystalline lithium mixed ferrimagnetic films. Chinese Journal of Physics, 39(6), 635-640.
6. Samarasekara, P., De Silva, S.N.P. (2007). Heisenberg Hamiltonian solution of thick ferromagnetic films with second-order perturbation. Chinese Journal of Physics, 45(2-I), 142.
7. Samarasekara, P., Saparamadu, U. (2013). In-plane oriented strontium ferrite thin films described by spin reorientation. Research & Reviews: Journal of Physics - STM Journals, 2(2), 12-16.
8. Samarasekara, P., Ekanayake, E.M.P. (2020). Ferromagnetic thin films with simple cubic structure as described by fourth-order perturbed Heisenberg Hamiltonian. STM Journals: Journal of Nanoscience, Nanoengineering & Applications, 10(3), 35-43.
9. Samarasekara, P., Mendoza, W.A. (2010). Effect of third order perturbation on

Heisenberg Hamiltonian for non-oriented ultra-thin ferromagnetic films. Electronic Journal of Theoretical Physics, 7(24), 197-210.

10. Samarasekara, P., Warnakulasooriya, B.I. (2016). Five layered FCC ferromagnetic films as described by modified second order perturbed Heisenberg Hamiltonian. Journal of Science of the University of Kelaniya, Sri Lanka, 11, 11-21.
11. Yapa, N.U.S., Samarasekara, P., Dehipawala, S. (2017). Variation of magnetic easy direction of BCC structured ferromagnetic films up to thirty spin layers. Ceylon Journal of Science, 46(3), 93.
12. Samarasekara, P., Abeyratne, M.K., Dehipawalage, S. (2009). Heisenberg Hamiltonian with second order perturbation for spinel ferrite thin films. Electronic Journal of Theoretical Physics, 6(20), 345.
13. Samarasekara, P. (2008). Influence of third order perturbation on Heisenberg Hamiltonian of thick ferromagnetic films. Electronic Journal of Theoretical Physics, 5(17), 227.
14. Hucht, A., Usadel, K.D. (1997). Reorientation transition of ultrathin ferromagnetic films. Physical Review B, 55, 12309.
15. Hucht, A., Usadel, K.D. (1999). Theory of the spin reorientation transition of ultra-thin ferromagnetic films. Journal of Magnetism and Magnetic Materials, 203(1), 88.
16. Usadel, K.D., Hucht, A. (2002). Anisotropy of ultrathin ferromagnetic films and the spin reorientation transition. Physical Review B, 66, 024419.
17. Samarasekara, P. (2006). Second order perturbation of Heisenberg Hamiltonian for non-oriented ultra-thin ferromagnetic films. Electronic Journal of Theoretical Physics, 3(11), 71.
18. Samarasekara, P. (2010). Determination of energy of thick spinel ferrite films using Heisenberg Hamiltonian with second order perturbation. GESJ: Physics, 1(3), 46–52.
19. Samarasekara, P. (2011). Investigation of third order perturbed Heisenberg Hamiltonian of thick spinel ferrite films. Inventi Rapid: Algorithm Journal, 2(1), 1–3.
20. Samarasekara, P., Ekanayake, E.M.P. (2021). Fourth order perturbed Heisenberg Hamiltonian of FCC structured ferromagnetic ultra-thin films. GESJ: Physics, 1(25), 19-29.
21. Samarasekara, P., Abeyratne, M.K. (2021). Magnetic properties of ferromagnetic thin films with three spin layers as described by fourth-order perturbed Heisenberg Hamiltonian. Journal of Science of the University of Kelaniya, Sri Lanka, 14, 31-50.